Character of Z-pole data constraints on standard model parameters

T. Kawamoto*

International Centre for Elementary Particle Physics, University of Tokyo, Tokyo 113-0033, Japan

R. G. Kellogg[†]

Department of Physics, University of Maryland, College Park, Maryland 20742, USA

Despite the impressive precision of the Z-pole measurements made at the e^+e^- colliders at CERN (LEP) and SLAC (SLC), the allowed region for the principal standard model parameters responsible for radiative corrections [m_H, m_t, and $\alpha(m_Z^2)$] is still large enough to encompass significant nonlinearities. The nature of the experimental constraints therefore depends in an interesting way on the ''accidental'' relationships among the various measurements. In particular, the fact that the Z-pole measurements favor values of m_H excluded by direct searches leads us to examine the effects of external Higgsstrahlung, a process ignored by the usual precision electroweak calculations.

I. INTRODUCTION

The precise measurements of Z resonance properties made by the four collaborations at the CERN e^+e^- collider LEP and by the SLAC Large Detector (SLD) at the SLC have confirmed all relevant predictions of the standard model and established a strong experimental basis for the mechanism of symmetry breaking in the electroweak sector. The two fundamental equations of electroweak unification,

$$\sin^2\theta_W = \frac{\pi\alpha}{\sqrt{2}m_W^2 G_F}, \qquad (1)$$

$$\cos^2\theta_W = \frac{m_W^2}{m_Z^2\rho_0}, \qquad (2)$$

establish the relations between the strengths of the electromagnetic and weak couplings, and the mass ratio of the neutral and charged heavy vector bosons. Here G_F is the Fermi constant determined in muon decay, α is the electromagnetic fine-structure constant, m_W and m_Z are the W and Z boson masses, and θ_W is the electroweak mixing angle. The ρ_0 parameter [1] is determined by the Higgs structure of the theory; in the minimal standard model which we consider here, ρ_0 is unity.

G_F, m_Z, and $\alpha(m_Z^2)$ are known with relative precisions of $(1, 2, \text{and } 40)\times10^{-5}$. This allows the radiative corrections to Eqs. (1) and (2) to be investigated in considerable detail. These radiative corrections depend principally on the masses of the top quark, m_t, and the Higgs boson, m_H. One of the great strengths of the Z-pole data is that the measurements of the partial widths and charge asymmetries allow the effects of the Higgs boson and the top quark to be separated to a remarkable extent. The character of this separation is the primary topic of this paper.

Since the top quark has been observed directly, the agreement between the directly measured mass and its indirect measurement derived through the radiative corrections provides compelling evidence that the theoretical and experimental understanding of the Z-pole measurements rests upon firm ground. The much smaller effects due to m_H then provide essentially the only experimental knowledge we have concerning this elusive particle, apart from the fact that it has so far escaped direct observation.

The broad range of m_H still consistent with the measurements provides sufficient room for nonlinear effects to become important. Such nonlinearities mean that the Gaussian error hypothesis, which is implicit in the χ^2 fits used to determine the error contours of the standard model parameters, approximates the true errors only imperfectly. The actual errors and even the shape of the measurement constraints depend significantly on the working point of the fit in the multidimensional space describing the range accessible to the parameters. The character of the m_t, m_H separation therefore depends in an interesting manner on the ''accidental'' relations between the various measurements. Variations on the scale of the expected measurement uncertainties can, in some cases, lead to disproportionate shifts in the error contours. In other cases, the specific manner in which a measurement happens to lie within its band of uncertainty results in unanticipated stability. Some understanding of these subtle effects is necessary for a full appreciation of the measurements.

Since we are interested in describing how our knowledge is augmented by each individual measurement as well as sets of measurements in combination, we are led naturally to consider hypothetical situations that explicitly violate constraints lying beyond the set of measurements being considered at any particular moment. Chief among the constraints we often ignore is the experimental lower limit on m_H provided by the direct searches [2]. A related complication in the analysis arises from what may be a historical accident. Due to the early and continued nonobservation of the Higgs boson at LEP, the two most precise electroweak programs ZFITTER [3–8] and TOPAZ0 [9–12] do not include the effects of external Higgs boson emission from the Z propagator. Since the

*Electronic address: tatsuo.kawamoto@cern.ch

[†]Electronic address: richard.kellogg@cern.ch

     69 113008-1

Z-pole measurements in fact favor a low-mass Higgs boson, we are led to consider the effects of such Higgsstrahlung in order to provide a self-consistent picture of what these measurements alone tell us about the standard model.

II. RADIATIVE CORRECTIONS

The largest radiative correction affecting the basic electroweak relations presented in the previous section is due to the running of the electromagnetic coupling constant in Eq. (1). This running is due to the presence of fermion loops in the photon propagator, and is usually parametrized as

$$\alpha(s) = \frac{\alpha(0)}{1 - \Delta\alpha(s)}. \tag{3}$$

Near the Z pole, leptons, the top quark, and the five light quarks contribute to $\Delta\alpha(s)$:

$$\Delta\alpha(s) = \Delta\alpha_{e\mu\,\tau}(s) + \Delta\alpha_{\mathrm{top}}(s) + \Delta\alpha_{\mathrm{had}}^{(5)}(s). \tag{4}$$

The Z-pole data themselves give no useful experimental constraints on $\Delta\alpha(s)$. The first two terms of Eq. (4) can be precisely calculated, but $\Delta\alpha_{\mathrm{had}}^{(5)}(s)$ is best determined by analyzing the measured rate of e^+e^- annihilation to hadrons using a dispersion relation [13], where low-energy data dominate the resulting uncertainty. At LEP and SLC energies, α is increased from the Thompson limit of 1/137.036 to 1/128.945, corresponding to $\Delta\alpha_{\mathrm{had}}^{(5)}(m_Z^2) = 0.02761 \pm 0.00036$ [13].

Combining Eqs. (1) and (2) and including radiative corrections yields

$$\cos^2\theta_{\mathrm{W}}\sin^2\theta_{\mathrm{W}} = \frac{\pi\alpha(0)}{\sqrt{2}m_Z^2 G_F} \frac{1}{1 - (\Delta\alpha + \Delta r_{\mathrm{w}})}, \tag{5}$$

where Δr_{w} represents further weak corrections. Equation (5) directly links $\Delta\alpha$ and Δr_{w} to the value of θ_{W}, and hence to m_{W} via Eq. (2).

Radiative corrections also affect the couplings of the Z to fermions. The bulk of these corrections [14] can be absorbed into an overall scale factor for the couplings, ρ_f, and a scale factor κ_f for the electroweak mixing angle, resulting in the "effective" quantities

$$\rho_f = 1 + \Delta\rho_{\mathrm{se}} + \Delta\rho_f, \tag{6}$$

$$\kappa_f = 1 + \Delta\kappa_{\mathrm{se}} + \Delta\kappa_f, \tag{7}$$

$$\sin^2\theta_{\mathrm{eff}}^f = \kappa_f\sin^2\theta_{\mathrm{W}}, \tag{8}$$

$$g_{\mathrm{V}f} = \sqrt{\rho_f}(T_f^3 - 2Q_f\sin^2\theta_{\mathrm{eff}}^f), \tag{9}$$

$$g_{\mathrm{A}f} = \sqrt{\rho_f}T_f^3. \tag{10}$$

Here T_f^3 is the third component of weak isospin, Q_f is the charge, θ_{eff}^f is the effective electroweak mixing angle, and $g_{\mathrm{V}f}$ and $g_{\mathrm{A}f}$ are the effective vector and axial-vector couplings for the fermion species f. The quantities $\Delta\rho_{\mathrm{se}}$ and

$\Delta\kappa_{\mathrm{se}}$ are universal corrections arising from the propagator self-energies, while $\Delta\rho_f$ and $\Delta\kappa_f$ are flavor-specific vertex corrections. The effective couplings $g_{\mathrm{V}f}$ and $g_{\mathrm{A}f}$ are purely real, and describe that part of the Z interaction which can be treated as a resonance in the improved Born approximation. The remaining, complex parts, termed "remnants," generate effects that are small compared to the experimental errors, but are nevertheless respected when determining $g_{\mathrm{V}f}$ and $g_{\mathrm{A}f}$ from the data (see, for example, [15]).

The Z partial width to each fermion species, $\Gamma_{f\bar{f}}$, is proportional to ρ_f, while $\sin^2\theta_{\mathrm{eff}}^{\mathrm{lept}}$, measured through the asymmetries, is proportional to κ_f. Calculations at one-loop order illustrate the essential m_{t} and m_{H} dependencies [16], which are quadratic in m_{t} and logarithmic in m_{H}. The dependence of $\Delta\kappa_{\mathrm{se}}$ remains the same over the entire range of m_{H}:

$$\Delta\kappa_{\mathrm{se}} = \frac{3G_F m_{\mathrm{W}}^2}{8\sqrt{2}\pi^2}\frac{m_{\mathrm{t}}^2}{m_{\mathrm{W}}^2}\frac{\cos^2\theta_{\mathrm{W}}}{\sin^2\theta_{\mathrm{W}}} - \frac{10}{3}\frac{G_F m_{\mathrm{W}}^2}{8\sqrt{2}\pi^2}\left(\ln\frac{m_{\mathrm{H}}^2}{m_{\mathrm{W}}^2} - \frac{5}{6}\right)$$
$$+ \cdots. \tag{11}$$

For $\Delta\rho_{\mathrm{se}}$, the sign of the dependence on $\ln(m_{\mathrm{H}})$ is negative for $m_{\mathrm{H}} \gg m_{\mathrm{W}}$,

$$\Delta\rho_{\mathrm{se}} = \frac{3G_F m_{\mathrm{W}}^2}{8\sqrt{2}\pi^2}\frac{m_{\mathrm{t}}^2}{m_{\mathrm{W}}^2} - \frac{3G_F m_{\mathrm{W}}^2}{8\sqrt{2}\pi^2}\frac{\sin^2\theta_{\mathrm{W}}}{\cos^2\theta_{\mathrm{W}}}\left(\ln\frac{m_{\mathrm{H}}^2}{m_{\mathrm{W}}^2} - \frac{5}{6}\right) + \cdots, \tag{12}$$

and positive for $m_{\mathrm{H}} \ll m_{\mathrm{W}}$,

$$\Delta\rho_{\mathrm{se}} = \frac{3G_F m_{\mathrm{W}}^2}{8\sqrt{2}\pi^2}\frac{m_{\mathrm{t}}^2}{m_{\mathrm{W}}^2} + \frac{G_F m_Z^2}{4\sqrt{2}\pi^2}\ln\frac{m_{\mathrm{H}}^2}{m_Z^2} - \frac{7G_F m_{\mathrm{H}} m_Z}{8\sqrt{2}\pi}\cdots. \tag{13}$$

Equation (8) shows that $\sin^2\theta_{\mathrm{eff}}^{\mathrm{lept}}$ receives radiative corrections both from Δr_{w}, through $\sin^2\theta_{\mathrm{W}}$, and from $\Delta\kappa_{\mathrm{se}}$ directly. These corrections act along the same axis in the m_{t} vs $\ln(m_{\mathrm{H}})$ plane, but in opposite senses due to the near equality, in single-loop approximation:

$$\Delta\kappa_{\mathrm{se}} = -\Delta r_{\mathrm{w}} + \cdots. \tag{14}$$

In the m_{t} vs $\ln(m_{\mathrm{H}})$ plane lines of constant $\Delta\kappa_{\mathrm{se}}$ and Δr_{w}, and hence m_{W} and $\sin^2\theta_{\mathrm{eff}}^{\mathrm{lept}}$, are therefore all approximately parallel. When moving along such lines, then, changes in the radiative effects of the top quark and the Higgs boson are seen to cancel. It is only through violations of this approximation that measurements of m_{W} and $\sin^2\theta_{\mathrm{eff}}^{\mathrm{lept}}$ have any power to separate the effects of m_{t} and m_{H}.

The fact that Δr_{w} and $\Delta\kappa_{\mathrm{se}}$ oppose each other in Eq. (8) reduces the sensitivity of $\sin^2\theta_{\mathrm{eff}}^{\mathrm{lept}}$ to the corrections. The effect of Δr_{w} is larger, so that changes in $\sin^2\theta_{\mathrm{eff}}^{\mathrm{lept}}$ are of the same sign as those in $\sin^2\theta_{\mathrm{W}}$, but are a factor of $\sin^2\theta_{\mathrm{W}}/\cos^2\theta_{\mathrm{W}}$ smaller in magnitude [17], which is about 0.3.

Since $\sin^2\theta_W$ is present in the dominant, m_t, term of Eq. (11), but absent in the corresponding terms of Eqs. (12) and (13), the effects of $\Delta\alpha_{\text{had}}^{(5)}(m_Z^2)$ are felt in $\Delta\kappa_{\text{se}}$, but $\Delta\rho_{\text{se}}$ is well isolated. The uncertainty in $\Delta\alpha_{\text{had}}^{(5)}(m_Z^2)$ therefore dilutes the inherent precision of the $\sin^2\theta_{\text{eff}}^{\text{lept}}$ measurements, but not those of the partial widths.

Similarly, the weak effects of Δr_w are felt undiluted in m_W, so that the relative effect of $\Delta\alpha$ is much smaller there than it is for $\sin^2\theta_{\text{eff}}^{\text{lept}}$, where about 0.7 of the weak corrections are canceled through $\Delta\kappa_{\text{se}}$.

The flavor dependence of the radiative corrections is very small for all fermions, except for the b quark, where vertex corrections are significant due to the large mass splitting between the bottom and top quarks [18], resulting in

$$\Delta\rho_b = -\frac{G_F m_t^2}{2\sqrt{2}\,\pi^2} + \cdots. \qquad (15)$$

Notice that $\Delta\rho_b$ has no Higgs boson dependence, making the quantity $R_b^0 = \Gamma_{b\bar{b}}/\Gamma_{\text{had}}$ a straight-forward indicator of m_t, since the m_H dependencies entering through $\Delta\rho_{\text{se}}$ cancel in the numerator and denominator.

The partial Z decay widths contain final state radiative corrections and add up straightforwardly to yield the total width of the Z boson [19]:

$$\Gamma_{\text{f}\bar{\text{f}}} = N_c^f \frac{G_F m_Z^3}{6\sqrt{2}\,\pi}(|\mathcal{G}_{\text{Af}}|^2 R_{\text{Af}} + |\mathcal{G}_{\text{Vf}}|^2 R_{\text{Vf}}) + \Delta_{\text{ew/QCD}}. \qquad (16)$$

Here the complex effective couplings $\mathcal{G}_{\text{Vf}}$ and $\mathcal{G}_{\text{Af}}$ differ only by small imaginary parts from the real effective couplings defined in Eqs. (9) and (10). The radiator factors R_{Vf} and R_{Af} take into account final state QED and QCD [20] corrections including pair production; $\Delta_{\text{ew/QCD}}$ accounts for small contributions from nonfactorizable electroweak-QCD corrections.

Although the discussion of electroweak corrections presented above [Eqs. (11)–(15)] is at the single-loop level, serious quantitative calculations implemented in programs such as ZFITTER and TOPAZ0 include terms of higher order. These programs can not only calculate the effective couplings as a function of the free standard model parameters, but can also relate these couplings to observables such as cross sections and partial widths. The simple single-loop expressions are nevertheless useful in understanding the results of the elaborate, very precise calculations used in deriving our quantitative results.

III. Z-POLE CONSTRAINTS ON m_t AND m_H

As Z-pole input data we consider the set listed in Table 16.1 of Ref. [21], which consists of $\Delta\alpha_{\text{had}}^{(5)}(m_Z^2)$, plus the 14 Z-pole measurements: m_Z, Γ_Z, σ_h^0, R_ℓ^0, $A_{\text{FB}}^{0,\ell}$, $\mathcal{A}_\ell(P_\tau)$, $\sin^2\theta_{\text{eff}}^{\text{lept}}(\langle Q_{\text{FB}}\rangle)$, $\mathcal{A}_\ell$ (SLD), R_b^0, R_c^0, $A_{\text{FB}}^{0,b}$, $A_{\text{FB}}^{0,c}$, $\mathcal{A}_b$, and $\mathcal{A}_c$, including their error correlations. We perform standard model fits[1] to these data, using ZFITTER 6.36 to predict the observables as a function of the five free parameters $\Delta\alpha_{\text{had}}^{(5)}(m_Z^2)$, m_Z, α_S, m_t, and m_H.

To illustrate the constraints imposed by these measurements, it is useful to group them according to their functional roles. Two quantities, $\Delta\alpha_{\text{had}}^{(5)}(m_Z^2)$ and m_Z, appear as both input data and fit parameters. The electromagnetic coupling, parametrized through $\Delta\alpha_{\text{had}}^{(5)}(m_Z^2)$, is determined externally [13], and passes through the Z-pole fit as an inert ingredient. Similarly, m_Z is determined with such precision that it is incapable of being pulled by its dynamic relation to other quantities. Both might just as well have been treated as external constants, like G_F. The b- and c-quark asymmetry parameters $\mathcal{A}_b$ and $\mathcal{A}_c$ are also inert in the fit, since they have essentially no dependence on the standard model parameters.

The three measurements Γ_Z, σ_h^0, and R_ℓ^0 are equivalent to the more meaningful but more correlated quantities $\Gamma_{\ell\ell}$, Γ_{had}, and $\Gamma_{\text{inv}}/\Gamma_{\ell\ell}$. Of these, the last is insensitive to variations in the standard model parameters and serves to measure the number of light neutrino generations. The strong coupling constant α_S is determined by its effect on the hadronic width Γ_{had}, leaving $\Gamma_{\ell\ell}$ as the key quantity in constraining $\Delta\rho_{\text{se}}$. The small size of $g_{V\ell}$ compared to $g_{A\ell}$ [see Eq. (9)] makes $\Gamma_{\ell\ell}$ essentially independent of $\sin^2\theta_{\text{eff}}^{\text{lept}}$.

As already discussed in connection with Eq. (15), R_b^0 serves as a direct indicator of m_t. The role of R_c^0 is diffuse and noncritical.

The six remaining measurements $A_{\text{FB}}^{0,\ell}$, $\mathcal{A}_\ell(P_\tau)$, $\sin^2\theta_{\text{eff}}^{\text{lept}}(\langle Q_{\text{FB}}\rangle)$, $\mathcal{A}_\ell$ (SLD), $A_{\text{FB}}^{0,b}$, and $A_{\text{FB}}^{0,c}$ serve to determine the single quantity $\sin^2\theta_{\text{eff}}^{\text{lept}}$. Although there is a disturbing lack of consistency between the values of $\sin^2\theta_{\text{eff}}^{\text{lept}}$ derived from the two most precise measurements $\mathcal{A}_\ell$ (SLD) and $A_{\text{FB}}^{0,b}$, the discrepancy[2] ($\approx 2.9\sigma$) between them appears to elude explanation. Within the standard model all six of these measurements, and particularly the two most precise, appear to be valid and well-defined measurements of $\sin^2\theta_{\text{eff}}^{\text{lept}}$.

Both measurements claim to be dominated by statistical uncertainties. The measurements [21] of $A_{\text{FB}}^{0,b}$ are complex, but the level of agreement between the independent analyses of the four LEP Collaborations is excellent. Common QCD corrections play a role, but are believed to be well understood. The SLD measurement [22] of $\mathcal{A}_\ell$ through A_{LR}, the asymmetry between the interaction rate for right- and left-handed electron beam polarizations, is both simple and elegant. The least implausible source of systematic error, in the measurement of the beam polarization, is believed to be small and well controlled.

Here we investigate the consequences of excluding either $\mathcal{A}_\ell$ (SLD) or $A_{\text{FB}}^{0,b}$ from the fit, but we make no attempt to choose between them. Either exclusion option restores ac-

---

[1]Our results are equivalent to those described in [21]. The resulting numerical values for the standard model parameters can be found in Table 16.2 of that reference.

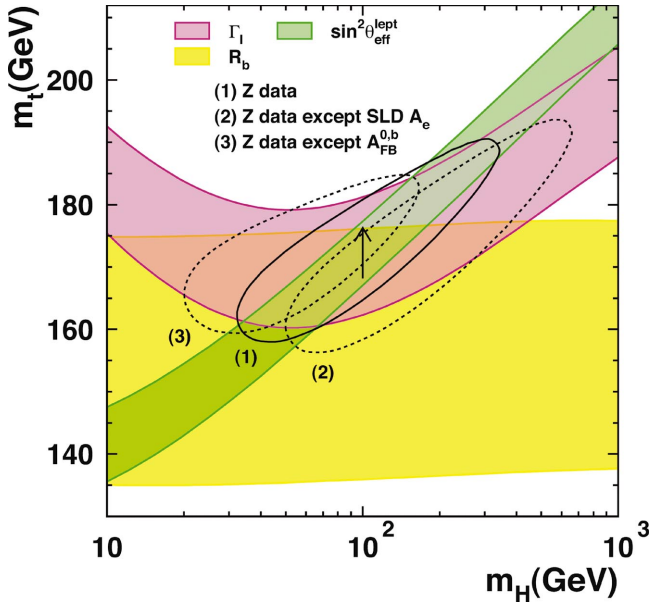[2]The $A_{\text{FB}}^{0,b}$ measurements are not yet final.

FIG. 1. (Color) m_t and m_H constraints from the Z-pole measurements. Each band gives the $\pm 1\sigma$ constraint from the indicated measurement. The arrow indicates the additional variation in $\sin^2\theta_{\rm eff}^{\rm lept}$ due to a $\pm 1\sigma$ uncertainty in $\Delta\alpha_{\rm had}^{(5)}(m_Z^2)$. The ellipses give the 68% C.L. fit contours for the indicated data.

ceptable consistency to the set of $\sin^2\theta_{\rm eff}^{\rm lept}$ measurements, but obviously introduces a bias.

The constraints on m_t and m_H imposed by the 14 Z-pole measurements can therefore be almost completely expressed in terms of three quantities: $\Gamma_{\ell\ell}$, related directly to $\Delta\rho_{\rm se}$; $\sin^2\theta_{\rm eff}^{\rm lept}$, related directly to $\Delta\kappa_{\rm se}$; and R_b^0, related directly to m_t.

A. Z-pole data constraints alone

How these components of the Z-pole data constrain m_t and m_H can be clearly illustrated on a plot of m_t vs $\log_{10}(m_H/{\rm GeV})$, as shown in Fig. 1. Shown here are the usual 68% C.L. error contours, plotted by finding the curve in the m_t vs $\log_{10}(m_H/{\rm GeV})$ plane where the χ^2 of the fit exceeds its minimum by 2.28. For projections in a single parameter, 68% C.L. corresponds to 1.51σ. Also plotted are measurement constraint bands, which show the contribution of each measurement. These are plotted by finding the curves in the m_t vs $\log_{10}(m_H/{\rm GeV})$ plane where the predicted value of the measured quantity equals the central value of the measurement $\pm 1\sigma$. Note that, since each of these bands indicates the constraint imposed by a fixed measurement, it exhibits exactly the inverse parameter dependence compared to the standard model prediction for the measured quantity.

The diagonal band in Fig. 1 indicates the $\pm 1\sigma$ constraint from the $\sin^2\theta_{\rm eff}^{\rm lept}$ measurements. Higher-order electroweak corrections do not significantly affect the linear relationship expected from the lowest-order terms, and the slope of this band is approximated by the ratio of the coefficients of m_t^2

and $\ln(m_H)$ in the expression for $\Delta\kappa_{\rm se}$:[3]

$$\left.\frac{dm_t}{d\ln(m_H)}\right|_{\kappa_{\rm se}} = \frac{10}{9}\frac{m_Z^2\sin^2\theta_{\rm W}}{m_t}. \tag{17}$$

The banana-shaped band in Fig. 1 shows the $\pm 1\sigma$ constraint from the $\Gamma_{\ell\ell}$ measurement. The slope of this band at large $\log_{10}(m_H/{\rm GeV})$ agrees reasonably with the linear relation expected from the ratio of coefficients in the lowest-order expression for $\Delta\rho_{\rm se}$ in this region:

$$\left.\frac{dm_t}{d\ln(m_H)}\right|_{\rho_{\rm se}} = \frac{m_Z^2}{m_t}\sin^2\theta_{\rm W}. \tag{18}$$

Also, at low $\log_{10}(m_H/{\rm GeV})$ the slope, now negative, agrees with the lowest-order expression given in Eq. (13):

$$\left.\frac{dm_t}{d\ln(m_H)}\right|_{\rho_{\rm se}} = -\frac{2m_Z^2}{3m_t}. \tag{19}$$

Due to the fact that R_b^0 is controlled by vertex corrections determined by the t-b mass splitting, its measurement provides a constraint on m_t almost independent of $\log_{10}(m_H/{\rm GeV})$, as shown by the broad horizontal band in Fig. 1 (also $\pm 1\sigma$).

The central ellipse in Fig. 1 shows the 68% C.L. contour for the standard model fit to all Z-pole measurements. The dominant role played by $\sin^2\theta_{\rm eff}^{\rm lept}$ in determining the minor axis is evident, and the turnover of the $\Gamma_{\ell\ell}$ banana provides the lower bound of the major axis. The R_b^0 measurement provides the upper bound. If the R_b^0 constraint is removed, the fit in fact no longer yields a 68% C.L. upper limit for m_H or m_t.

The other two ellipses in Fig. 1 show similar fit contours when either the $A_{\rm LR}$ or the $A_{\rm FB}^{0,b}$ measurements are excluded from the fit. The noticeable shrinkage of the major axis in the case when the $A_{\rm FB}^{0,b}$ measurement is dropped is due to the fact that the $\sin^2\theta_{\rm eff}^{\rm lept}$ constraint then begins to move around the corner of the $\Gamma_{\ell\ell}$ banana. If the $\sin^2\theta_{\rm eff}^{\rm lept}$ measurement moved even lower in m_H, the $\sin^2\theta_{\rm eff}^{\rm lept}$ and $\Gamma_{\ell\ell}$ constraints would become almost perpendicular, eliminating the usual m_t-$\log_{10}(m_H/{\rm GeV})$ error correlation.

The agreement of the indirect measurement of m_t from the Z-pole measurements alone with the direct measurement made in $p\bar{p}$ collisions [23] ($m_t = 174.3 \pm 5.1$ GeV) is an important experimental confirmation of the validity of electroweak corrections. The remarkable stability of the indirect measurement's central value under shifts in $\sin^2\theta_{\rm eff}^{\rm lept}$ can be seen to result from a complex interplay between the relatively weak constraint from R_b^0, which happens to lie low, and the exact relation between the $\sin^2\theta_{\rm eff}^{\rm lept}$ measurement band and the position of the $\Gamma_{\ell\ell}$ corner.

---

[3]Note that the success of this approximation relies on $\Delta r_{\rm w}$ remaining constant along lines of constant $\sin^2\theta_{\rm eff}^{\rm lept}$, as mentioned in the text discussing Eq. (14).

The arrow in Fig. 1 shows how the $\sin^2\theta_{\text{eff}}^{\text{lept}}$ measurement band would shift under a $\pm1\sigma$ change in the $\Delta\alpha_{\text{had}}^{(5)}(m_Z^2)$ determination. Only the $\sin^2\theta_{\text{eff}}^{\text{lept}}$ measurement is significantly sensitive to $\Delta\alpha_{\text{had}}^{(5)}(m_Z^2)$ on the scale of the current errors, making the effective width of the $\sin^2\theta_{\text{eff}}^{\text{lept}}$ measurement band in the m_t vs m_H plane about 50% wider than the band shown, which corresponds to $\Delta\alpha_{\text{had}}^{(5)}(m_Z^2)$ fixed at its central value.

The effect of applying the constraint of the direct m_t measurement [23] can easily be visualized by imagining a horizontal band at $m_t = 174.3 \pm 5.1$ GeV. Notice that at the operating point of the Z-pole fit, the direct m_t measurement essentially surplants not only R_b^0, but also the constraints provided by $\Gamma_{\ell\ell}$.

It is perhaps interesting to remark on the fact that all measurements are compatible with the broad $\Gamma_{\ell\ell}$ extremum in $\log_{10}(m_H/\text{GeV})$. Only the failure to find direct production of the Higgs boson at LEP II indicates nature's choice to lie on the $\Gamma_{\ell\ell}$ upper branch.

B. Additional constraints from m_W

Direct measurements of m_W also provide important constraints on the standard model parameters through the electroweak corrections Δr_w. The high precision of the m_Z measurement means that the constraint imposed on $\sin^2\theta_W$ through Eq. (2) is effectively limited only by the measurement uncertainty in m_W. Although further precision on m_W from both LEP II [21] and the Tevatron [24] can be expected, the available combined result $m_W = 80.426 \pm 0.034$ GeV [21] is already sufficient to provide constraints on m_t and m_H that are comparable in precision to those derived from the Z pole alone. The approximate equivalence $\Delta r_w \approx -\Delta\kappa_{\text{se}}$ of Eq. (14) becomes less exact toward small values of m_H, so that the direct m_W measurements allow some separation of Higgs boson and top quark effects when combined with the Z-pole measurement of $\sin^2\theta_{\text{eff}}^{\text{lept}}$.

The diagonal m_W band in Fig. 2 shows the constraint from the preliminary direct measurements of m_W. The flattening of its slope at low values of m_H, and the fact that it happens to lie relatively higher in m_t than the $\sin^2\theta_{\text{eff}}^{\text{lept}}$ band, leads to a clear divergence of the two measurement bands at low m_H.

Compared to the solid error contour of the Z-pole fit without m_W, which is shown again in Fig. 2, the dashed error contour which includes the m_W measurements is displaced along the converging m_W and $\sin^2\theta_{\text{eff}}^{\text{lept}}$ measurement bands like the slider of a zipper toward larger values of m_t and m_H. This demonstrates that the m_W measurement provides a stronger lower bound along this axis than does $\Gamma_{\ell\ell}$.

The contour including m_W is also displaced perpendicularly and is therefore more compatible with the lower value of $\sin^2\theta_{\text{eff}}^{\text{lept}}$ derived from A_{LR} than the higher value favored by $A_{FB}^{0,b}$ (see Fig. 1).

Without constraining m_t it is the first displacement, parallel to the $\sin^2\theta_{\text{eff}}^{\text{lept}}$ band, which dominates, and the addition of m_W shifts the favored range for m_H upward, as already mentioned, with respect to the Z-pole-only fit.

When the direct measurement of $m_t = 174.3 \pm 5.1$ GeV is imposed at the outset, however, not only is m_H constrained
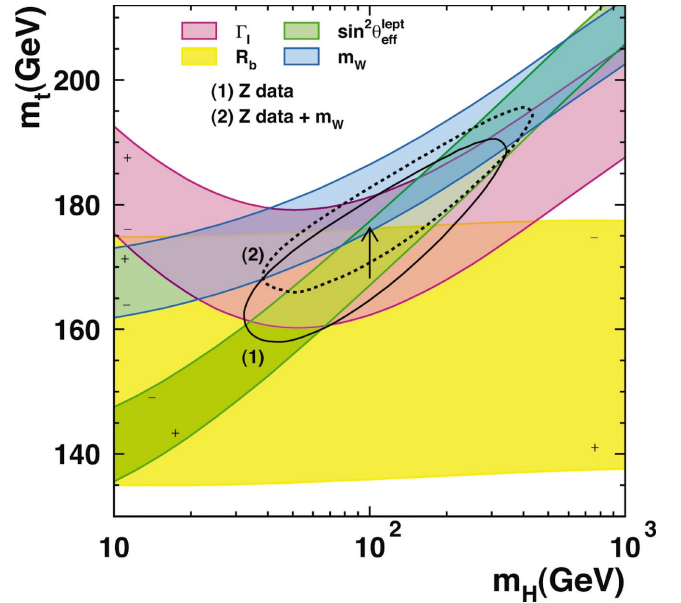

FIG. 2. (Color) m_t and m_H constraints from Z-pole measurements and m_W. Each band gives the $\pm1\sigma$ constraint from the indicated measurement. The $\pm$ signs on each band show the sense of variation in the measurement. The arrow indicates the additional variation in $\sin^2\theta_{\text{eff}}^{\text{lept}}$ due to a $\pm1\sigma$ uncertainty in $\Delta\alpha_{\text{had}}^{(5)}(m_Z^2)$. The error contours are shown at 68% C.L. for fits to both the Z-pole results alone (solid) and the Z-pole results combined with m_W (dashed).

more tightly, but the second, perpendicular displacement of the error ellipse then dominates, and the addition of m_W shifts the favored range for m_H downward, rather than upward.

IV. HIGGSSTRAHLUNG

Since direct searches for the Higgs boson have demonstrated that $m_H > 114$ GeV at 95% C.L. [2], Figs. 1 and 2 and Eq. (13) follow the precision calculations of ZFITTER and TOPAZ0 in neglecting the Higgsstrahlung process shown in Fig. 3. However, the decrease of $\Delta\rho_{\text{se}}$ at low m_H predicted by Eq. (13) is due to the effect of virtual Higgs boson loops. These should properly be compensated by external Higgs boson corrections, which will enter with opposite sign. When choosing to ignore the direct Higgs boson search results to
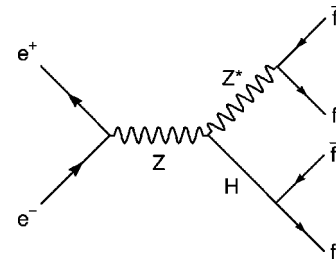

FIG. 3. Higgsstrahlung at the Z-pole. The narrow width of the Higgs boson implies that its decay products have an invariant mass near m_H, while the Z^* is sufficiently off shell to ensure energy conservation.
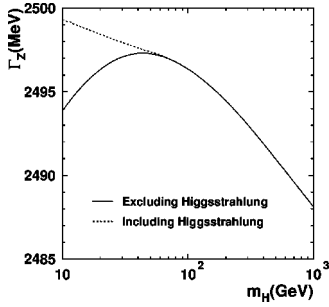
FIG. 4. Γ_Z vs $\log_{10}(m_H/\text{GeV})$, including and excluding external Higgsstrahlung.

explore what the Z-pole measurements alone tell us about the standard model, it is logically inconsistent to consider virtual Higgs boson corrections while neglecting the concomitant external corrections that the standard model predicts for low values of m_H.

We have therefore undertaken calculations that account for the effects of the expected Higgsstrahlung at low m_H. The fractional rate of such Higgsstrahlung is given in [16]:

$$\frac{\Gamma(Z \to H f\bar{f})}{\Gamma(Z \to f\bar{f})} = \frac{\alpha}{4\pi \cos^2\theta_W \sin^2\theta_W}$$

$$\times \int_{2r}^{1+r^2} \frac{(1 + 2r^2/3 - x + x^2/12)\sqrt{x^2 - 4r^2}}{[\Gamma_Z^2/m_Z^2 + (x - r^2)^2]}\,dx,$$

(20)

where

$$x = 2E_H/m_Z,$$ (21)

$$r = m_H/m_Z,$$ (22)

$$E_H = \frac{m_Z^2 + m_H^2 - m_{f\bar{f}}^2}{2m_Z},$$ (23)

and $m_{f\bar{f}}$ is the invariant mass of the Z^* decay products. The Higgsstrahlung of Eq. (20) represents extra width for Z decay, which is not included in ZFITTER. Figure 4 shows the total width of the Z with and without this external Higgsstrahlung. At values of m_H below ~ 50 GeV, which are still consistent with the Z-pole measurements, the standard model Higgsstrahlung would have been appreciable, representing on the order of 1 MeV in the Z decay width.

In order to incorporate the effects of such Higgsstrahlung into the Z-pole analysis, we reinterpret the experimental measurements, which we consider to include Higgsstrahlung, in terms of the theoretical quantities as calculated by ZFITTER, without Higgsstrahlung. In the case of the total width this is particularly straightforward:

$$\Gamma_Z^{\text{meas}} = \Gamma_Z^{\text{zf}} + \Gamma_Z^{\text{hs}},$$ (24)

where the superscripts have the obvious meanings: zf = ZFITTER, meas = measured, hs = Higgsstrahlung. Here Γ_Z^{hs}

$= \Gamma(Z \to H f\bar{f})$, summed over all fermion species, is calculated according to Eq. (20). Since Γ_Z is the resonance width of the Z, determined by the decay lifetime and the uncertainty principle, its measurement is entirely independent of any details of the experimental event selection and analysis.

The manner in which the measurement of the partial widths will be affected is less obvious. Although experimental details differ among the four LEP Collaborations, we take OPAL as a representative experiment [15,25] and study how Higgsstrahlung would have affected the measurements. Although it would be better to pursue these studies using detailed simulations of all four experiments, the precision that is necessary is sharply reduced by a very simple consideration: any Higgsstrahlung events classed as hadronic Z decays will simply increase the apparent value of α_S and will otherwise not affect the analysis. This is the case since, while Γ_{had} and $\Gamma_{\ell\ell}$ share the same propagator corrections through $\Delta\rho_{\text{se}}$, final-state QCD radiation increases the hadronic width alone by the factor R_{QCD}:

$$R_{\text{QCD}} = 1 + \frac{\alpha_S}{\pi} + \cdots.$$ (25)

Any shift in the $\Gamma_{\text{had}}/\Gamma_{\ell\ell}$ ratio is therefore interpreted by the fit as a change in α_S.

All four LEP experiments followed the natural strategy of essentially, if not formally, accepting all Z decays as hadronic unless they passed the stringent requirements to be identified as one of the three species of leptons. To an excellent approximation all Higgsstrahlung events in which the Z^* decays hadronically will remain classed as hadronic events. Since the dominant branching fraction of the Higgs boson in the relevant mass range is to $b\bar{b}$, many other Higgsstrahlung events, except for very low values of m_H, will also appear to be hadronic decays.

To clarify the experimental classification of the Higgsstrahlung events in which the Z^* decays leptonically we studied samples of fully simulated Higgstrahlung events in the OPAL detector. These samples were generated using the program HZHA-03 [26], included all accessible Higgs boson decays according to the standard model, and covered the Z^* decay channels e^+e^-, $\mu^+\mu^-$, and $\nu\bar{\nu}$. Since Z^* decays to $\tau^+\tau^-$ were not available, we treated these as an average of e^+e^- and $\mu^+\mu^-$.

For each Z^* decay channel, as a function of m_H, we calculated the probability that the Higgstrahlung events would be classified as hadronic Z decays. If an event failed the hadronic selection, we assumed that it would be classified correctly according to the actual Z^* decay. Since the standard model assumes lepton universality, any crossover between charged lepton channels would in any case be irrelevant.

We then calculated, as a function of m_H, two fractions: the fraction of Higgsstrahlung events $F^{\text{had}}\ell\ell(m_H)$ in which the Z^* in fact decayed to charged leptons, but the event was identified as an hadronic Z decay; and the fraction of
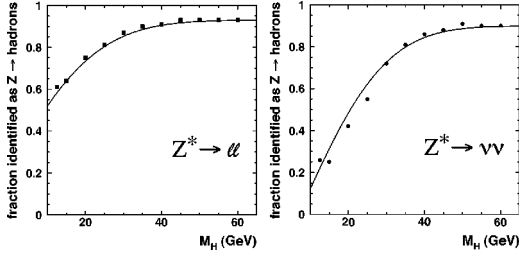
FIG. 5. As a function of m_H, the fractions of Higgsstrahlung events where the Z^* in fact decayed, respectively, to charged leptons or neutrinos, but the event was identified as a hadronic Z decay.

Higgsstrahlung events $F^{had}_{inv}(m_H)$ in which the Z^* in fact decayed to neutrinos, but the event was identified as a hadronic Z decay.

Figure 5 displays these fractions along with a smooth function fitted to represent the Monte Carlo data.

We then calculate the measured partial widths, including the effects of Higgsstrahlung, using the smooth F^{had}_{xx} functions:

$$\Gamma^{meas}_{had} = \Gamma^{zf}_{had} + F^{had}_{\ell\ell}(m_H)\Gamma^{hs}_{\ell\ell} + F^{had}_{inv}(m_H)\Gamma^{hs}_{inv}, \qquad (26)$$

$$\Gamma^{meas}_{\ell\ell} = \Gamma^{zf}_{\ell\ell} + [1 - F^{had}_{\ell\ell}(m_H)]\Gamma^{hs}_{\ell\ell}, \qquad (27)$$

$$\Gamma^{meas}_{inv} = \Gamma^{zf}_{inv} + [1 - F^{had}_{inv}(m_H)]\Gamma^{hs}_{inv}. \qquad (28)$$

We take the effect of Higgsstrahlung on the measurement of $\sin^2\theta^{lept}_{eff}$ to be negligible. Clearly there is no effect on the SLD measurement of A_{LR}, since it concerns only the initial state. Similarly, there can be no effect on the average τ polarization. The asymmetry measurements have a relative precision of at best a few percent, and any possible dilution of the asymmetry due to kinematic distortions in the few 10^{-3} fraction of Higgsstrahlung events will not be significant.

With the relations of Eqs. (24) and (26)–(28), we then remade the plot of Fig. 1, using ZFITTER to calculate the measurement error bands and 68% C.L. contours for the re-interpreted measurements. The result is shown in Fig. 6. Notice that the only visible change is the expected decrease in the slope of the $\Gamma_{\ell\ell}$ measurement band at low m_H, due to failure of some leptonic Higgsstrahlung events to be identified as hadrons. The lower extremity of the 68% C.L. contour for the fit which drops the $A^{0,b}_{FB}$ measurement extends very slightly, reflecting the local shift in the $\Gamma_{\ell\ell}$ constraint. The lower 1σ error on m_t is only 2.4% larger than it was when Higgsstrahlung was ignored. As a test of our procedures, we also carried out the same calculations assuming that all Higgsstrahlung was accepted as hadronic Z decay. As expected, the resulting plot was indistinguishable from Fig. 1.

In order to quantify the effect on α_S of Higgsstrahlung being identified as hadronic Z decay, we performed a series of four-parameter fits, with α_S, $\alpha(m^2_Z)$, m_Z, and m_t free, for a series of fixed m_H values. We plot the 1σ error bands of α_S as a function of $\log_{10}(m_H/\text{GeV})$ in Fig. 7, showing how α_S shifts to compensate for the Higgsstrahlung which is identified as hadronic Z decay. Since Γ^{zf}_{had}, the hadronic width as
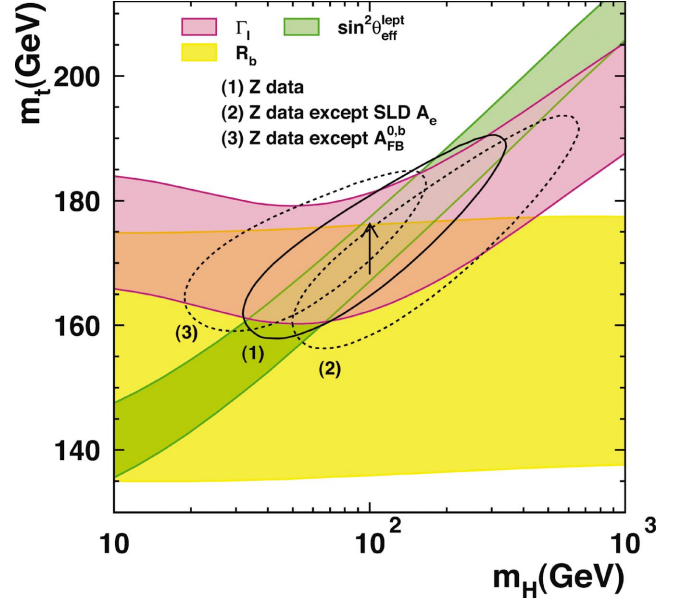

FIG. 6. (Color) m_t and m_H constraints from Z-pole measurements with Higgsstrahlung taken into account. Each band gives the $\pm 1\sigma$ constraint from the indicated measurement. The arrow indicates the additional variation in $\sin^2\theta^{lept}_{eff}$ due to a $\pm 1\sigma$ uncertainty in $\Delta\alpha^{(5)}_{had}(m^2_Z)$. The ellipses give the 68% C.L. fit contours for the indicated data.

reinterpreted for ZFITTER, is reduced from the fixed measured value Γ^{meas}_{had} by the Higgsstrahlung contribution, the hadronic final-state correction appears smaller, and the fit value of α_S is reduced as m_H becomes small.

The R^0_b measurement band remains unchanged in Fig. 6, since we have assumed that the Higgsstrahlung events identified as hadrons do not disturb the quark flavor balance. Ac-
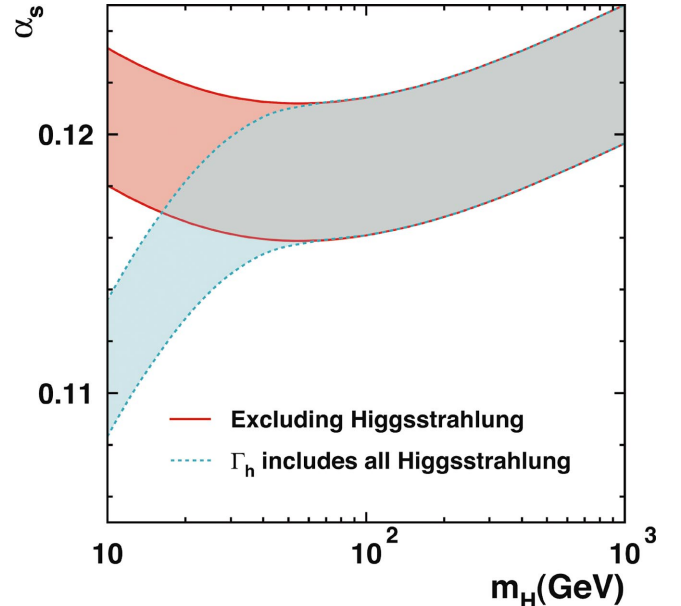

FIG. 7. (Color) The $\pm 1\sigma$ error bands for α_S found in the four-parameter fits as a function of $\log_{10}(m_H/\text{GeV})$, with and without Higgsstrahlung.
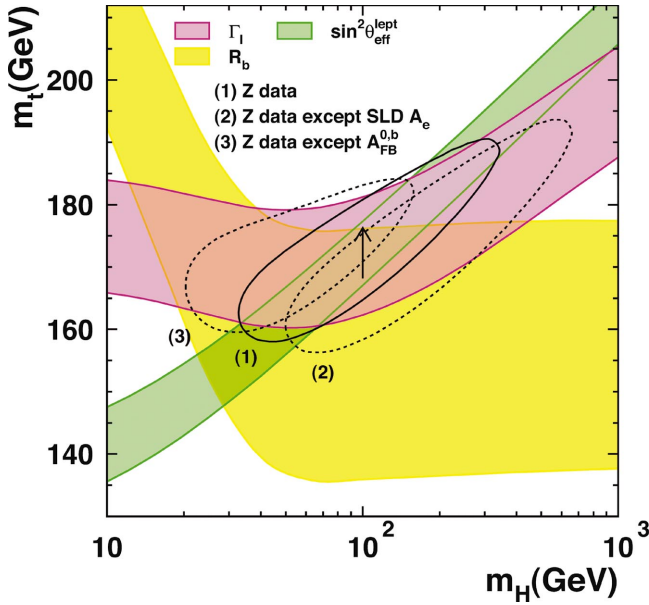
FIG. 8. (Color) m_t and m_H constraints from Z-pole measurements with Higgsstrahlung taken into account. Here the assumption is made that all Higgsstrahlung identified as hadrons contributes to $\Gamma_{b\bar{b}}$. Each band gives the $\pm 1\sigma$ constraint from the indicated measurement. The arrow indicates the additional variation in $\sin^2\theta_{\text{eff}}^{\text{lept}}$ due to a $\pm 1\sigma$ uncertainty in $\Delta\alpha_{\text{had}}^{(5)}(m_Z^2)$. The ellipses give the 68% C.L. fit contours for the indicated data.

tually, since the Higgs boson decays predominantly to $b\bar{b}$, it is likely that Higgsstrahlung will increase $\Gamma_{b\bar{b}}$ proportionally more than the width of other flavors. A complete heavy flavor analysis was beyond the scope of this study, so we considered the limiting case that all Higgsstrahlung events where the Higgs boson decays to $b\bar{b}$, and which are identified as hadrons, contribute to $\Gamma_{b\bar{b}}$:

$$\Gamma_{b\bar{b}}^{\text{meas}} = \Gamma_{b\bar{b}}^{\text{zf}} + \text{BR}(\text{Higgs} \to b\bar{b})[F_{\ell\ell}^{\text{had}}(m_H)\Gamma_{\ell\ell}^{\text{hs}}$$
$$+ F_{\text{inv}}^{\text{had}}(m_H)\Gamma_{\text{inv}}^{\text{hs}}]. \qquad (29)$$

The result is shown in Fig. 8.

The resulting dramatic upturn in the $\Gamma_{b\bar{b}}$ measurement band flattens the lower extremity of the 68% C.L. contour for

the Z-pole fit in which the $A_{\text{FB}}^{0,\text{b}}$ measurement is dropped, but only modestly. The lower 1σ error on m_t for this fit is 11% smaller than it was when Higgsstrahlung was ignored. The corresponding shift in the lower 1σ error on m_t for the base fit including all Z-pole measurements is only 1.7%. Other aspects of the error contours remain numerically unaffected.

V. CONCLUSIONS

Our study of the manner in which the Z-pole measurements constrain the standard model parameters m_t and m_H through their effect on radiative corrections shows that the measured leptonic width $\Gamma_{\ell\ell}$ plays an important and nonlinear role. This nonlinearity at low values of m_H contributes to a surprising stability in the agreement between the direct and indirect measurements of m_t under variations in $\sin^2\theta_{\text{eff}}^{\text{lept}}$. This singular demonstration of the consistency of our experimental and theoretical understanding of electroweak radiative corrections therefore remains undisturbed by the apparent discrepancy between the values of $\sin^2\theta_{\text{eff}}^{\text{lept}}$ derived from the measurements of $A_{\text{FB}}^{0,\text{b}}$ and A_{LR}.

The neglect of external Higgsstrahlung in ZFITTER and TO-PAZ0 in the analysis of the Z-pole measurements is found to have negligible impact on the central values of all the extracted standard model parameters, with the exception of α_S. Within a C.L. of 68% the error contours of these parameters also remain essentially unaffected.

[1] D.A. Ross and M.J.G. Veltman, Nucl. Phys. **B95**, 135 (1975).

[2] R. Barate *et al.*, Phys. Lett. B **565**, 61 (2003).

[3] D.Y. Bardin, M.S. Bilenkii, G. Mitselmakher, T. Riemann, and M. Sachwitz, Z. Phys. C **44**, 493 (1989).

[4] D.Y. Bardin, M.S. Bilenkii, T. Riemann, M. Sachwitz, and H. Vogt, Comput. Phys. Commun. **59**, 303 (1990).

[5] D.Y. Bardin *et al.*, Nucl. Phys. **B351**, 1 (1991).

[6] D.Y. Bardin *et al.*, Phys. Lett. B **255**, 290 (1991).

[7] D.Y. Bardin *et al.*, "Zfitter: An Analytical Program for Fermion Pair Production in e^+e^- Annihilation," hep-ph/9412201.

[8] D.Y. Bardin *et al.*, Comput. Phys. Commun. **133**, 229 (2001), recently updated with results from [27].

[9] G. Montagna, F. Piccinini, O. Nicrosini, G. Passarino, and R. Pittau, Nucl. Phys. **B401**, 3 (1993).

[10] G. Montagna, F. Piccinini, O. Nicrosini, G. Passarino, and R. Pittau, Comput. Phys. Commun. **76**, 328 (1993).

[11] G. Montagna, O. Nicrosini, G. Passarino, and F. Piccinini, Comput. Phys. Commun. **93**, 120 (1996).

[12] G. Montagna, O. Nicrosini, F. Piccinini, and G. Passarino, Comput. Phys. Commun. **117**, 278 (1999), recently updated to include initial state pair radiation [G. Passarino (private communication)]; hep-ph/9804211.

[13] H. Burkhardt and B. Pietrzyk, Phys. Lett. B **513**, 46 (2001).

[14] M.J.G. Veltman, Nucl. Phys. **B123**, 89 (1977).

[15] OPAL Collaboration, G. Abbiendi *et al.*, Eur. Phys. J. C **19**, 587 (2001).

[16] P. J. Franzini and P. Taxil, in *Z Physics At LEP1. Proceedings, Workshop, Geneva, Switzerland, 1989*, Vol. 2: Standard Physics, CERN 89-08, edited by G. Altarelli, R. Kleiss, and C. Verzegnassi (CERN, Geneva, Switzerland, 1989), p. 84.

[17] F. Jegerlehner, Prog. Part. Nucl. Phys. **27**, 1 (1991).

[18] F. Jegerlehner, in *Testing the Standard Model—TASI-90, Proceedings: Theoretical Advanced Study Institute in Elementary Particle Physics, Boulder, Colorado, 1990*, edited by M. Cvetic and P. Langacker (World Scientific, Singapore, 1991), p. 916.

[19] D.Y. Bardin, M. Grünewald, and G. Passarino, "Precision Calculation Project Report," hep-ph/9902452.

[20] K. Chetyrkin *et al.*, in *Reports of the Working Group on Precision Calculations for the Z Resonance, CERN 95-03*, edited by D. Bardin, W. Hollik, and G. Passarino (CERN, Geneva, Switzerland, 1995), p. 175.

[21] LEP Collaborations, the LEP Electroweak Working Group, and the SLD Electroweak and Heavy Flavour Groups, "A Combination of Preliminary Electroweak Measurements and Constraints on the Standard Model," hep-ex/0312023.

[22] SLD Collaboration, K. Abe *et al.*, Phys. Rev. Lett. **86**, 1162 (2001).

[23] Particle Data Group, K. Hagiwara *et al.*, Phys. Rev. D **66**, 010001 (2002).

[24] "Combination of CDF and DØ Results on *W* Boson Mass and Width," Tevatron Electroweak Working Group, CDF Collaboration, and DØ Collaboration, CDF Note No. 5888, DØ Note No. 3963, FERMILAB-FN-0716, 2002.

[25] OPAL Collaboration, K. Ahmet *et al.*, Nucl. Instrum. Methods Phys. Res. A **305**, 275 (1991).

[26] P. Janot, in *Physics at LEP, CERN 96-01, Vol. 2*, edited by T.S.G. Altarelli and F. Zwirner (CERN, Geneva, Switzerland, 1989), p. 309; for a description of the updates and for the code see http://alephwww.cern.ch/~janot/Generators.html

[27] A.B. Arbuzov, "Light Pair Corrections to Electron Positron Annihilation at LEP/SLC," hep-ph/9907500.